JACS
JOURNAL OF THE AMERICAN CHEMICAL SOCIETY

ARTICLE

pubs.acs.org/JACS

Transduction of Glycan−Lectin Binding Using Near-Infrared Fluorescent Single-Walled Carbon Nanotubes for Glycan Profiling

Nigel F. Reuel,[†] Jin-Ho Ahn,[†] Jong-Ho Kim,[‡] Jingqing Zhang,[†] Ardemis A. Boghossian,[†] Lara K. Mahal,[§] and Michael S. Strano*[,†]

[†]Department of Chemical Engineering, Massachusetts Institute of Technology, Cambridge, Massachusetts 02139, United States

[‡]Department of Chemical Engineering, Hanyang University, Ansan 426-791, Republic of Korea

[§]Department of Chemistry, New York University, New York, New York 10003, United States

Supporting Information

ABSTRACT: There is significant interest in developing new detection platforms for characterizing glycosylated proteins, despite the lack of easily synthesized model glycans or high affinity receptors for this analytical problem. In this work, we demonstrate a sensor array employing recombinant lectins as glycan recognition sites tethered via Histidine tags to Ni^{2+} complexes that act as fluorescent quenchers for semiconducting single-walled carbon nanotubes (SWNTs) embedded in a chitosan hydrogel spot to measure binding kinetics of model glycans. We examine, as model glycans, both free and streptavidin-tethered biotinylated monosaccharides. Two higher-affined glycan−lectin pairs are explored: fucose (Fuc) to PA-IIL and *N*-acetylglucosamine (GlcNAc) to GafD. The dissociation constants (K_D) for these pairs as free glycans (106 and 19 μM, respectively) and streptavidin-tethered (142 and 50 μM respectively) were found. The absolute detection limit for the current platform was found to be 2 μg of glycosylated protein or 100 ng of free glycan to 20 μg of lectin. Glycan detection (GlcNAc-streptavidin at 10 μM) is demonstrated at the single nanotube level as well by monitoring the fluorescence from individual SWNT sensors tethered to GafD lectin. Over a population of 1000 nanotubes, 289 of the SWNT sensors had signals strong enough to yield kinetic information (K_D of 250 ± 10 μM). We are also able to identify the locations of "strong transducers" on the basis of dissociation constant (four sensors with K_D < 10 μM) or overall signal modulation (eight sensors with >5% quench response). We report the key finding that the brightest SWNTs are not the best transducers of glycan binding. SWNTs ranging in intensity between 50 and 75% of the maximum show the greatest response. The ability to pinpoint strong-binding, single sensors is promising to build a nanoarray of glycan−lectin transducers as a high throughput method to profile glycans without protein labeling or glycan liberation pretreatment steps.

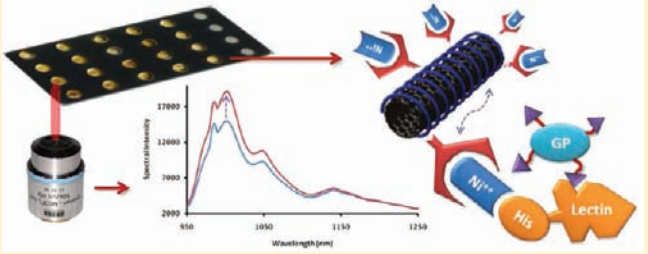

1. INTRODUCTION

Understanding the interactions between glycans and carbohydrate recognition domains (CRDs) found on cellular and protein surfaces is vital to the fields of glycobiology, immunology, and pharmacology. Glycans decorating the surface of proteins substantially influence function, such as folding pathways, signaling, retention, and pharmacokinetics.[1,2] The efficacy of protein-based therapeutics is largely dictated by their glycosylation,[3] and thus *de novo* design of drugs that interact with known CRD sites, such as cell-adhesion modulating galectins,[4] requires a greater understanding of the kinetic parameters between glycans and CRDs. Despite this importance, robust assays of protein glycosylation are underdeveloped, with the dominant profiling technologies falling to frontal affinity chromatography[5,6] and mass spectrometry.[7−9] Recently, the concept of the lectin microarray has emerged as a promising approach to investigating glycan-lectin interactions. These arrays take advantage of multivalent interactions to overcome the weak monovalent binding of lectin-glycan pairs (typically 10^{-7} M < K_d < 10^{-3} M) but are limited in their ability to transduce weak mono- or multivalent interactions and also require fluorescence labeling.[5,10−14] An emerging concept[5,10] is to use multivariate responses of glycan binding to a library of lectins to discern their identity, but this requires detection methods that are necessarily sensitive enough to transduce the presence of weakly bound proteins. Label-free methods, which reduce sample volume requirements, have a distinct advantage in this approach by decreasing the absolute detection limit. Herein, we develop a fluorescent single-walled carbon nanotube (SWNT) sensor[15] for glycan−lectin interactions with the ultimate goal of profiling glycans.

Our approach is to couple band gap fluorescent SWNTs to receptor lectins, which are a host of naturally occurring carbohydrate binding proteins.[16] We benchmark the sensor by evaluating the kinetic parameters between the anti-His tag antibody and comparing it to literature surface plasmon resonance (SPR) parameters. We then demonstrate the detection of fucose (Fuc)

Received: August 16, 2011
Published: October 04, 2011

to PA-IIL lectin and *N*-acetylglucosamine (GlcNAc) to GafD lectin. Kinetic parameters are obtained by first measuring the fluorescence intensity of a large spot of SWNT, and then it is shown how the same signal can be increased by probing individual SWNT sensors and determining which sensors are most responsive to glycosylated analyte addition. Our objective of glycan profiling makes this effort distinct from recent work creating glycosolate carbon nanotubes for therapeutic purposes[17,18] and electronic FET sensors for lectin, but not glycan, binding.[19−21] In contrast, the aim of our work is to profile glycans via their selective binding to a fluorescent nanotube surface, a concept not yet demonstrated in the literature to date.

Kinetic information on glycans−CRD interactions is currently determined by two types of analytical methodology: equilibrium and nonequilibrium.[22] Nonequilibrium methods yield relative binding information rather than physical kinetic rates; that is, they specify which glycan−CRD combinations bind with greater or lesser affinity in reference to each other. These methods include ELISA,[23] glycan microarrays,[24] agglutination,[25] and electrophoresis.[26] A notable exception in this category of relative binding assays are some of the carbohydrate arrays from the CH Wong group that can yield quantitative fluorescent binding curves similar to SPR (below) and be translated to K_D values.[14] Equilibrium dialysis can determine the forward reaction rate (k_f) of glycan−CRD binding but requires a large amount of glycan reagent, which is often a significant investment of time and money if complex sugars are used. Equilibrium titration calorimetry[27,28] is a delicate technique to determine kinetic parameters from thermodynamic information but is rarely employed because of time and reagent expenses. Another equilibrium technique, frontal affinity chromatography,[29] can be used to determine the affinity constant (K_D) for most glycan−CRD pairs ($K_D > 10^{-7}$); however the glycan must be labeled for detection. The current standard for obtaining kinetic information from label-free groups is surface plasmon resonance (SPR) machines, such as the Biacore systems. In the case of glycan−CRD interactions, SPR can detect both the forward and reverse kinetic rates for a wide range of affinities (K_D: mM−pM range). However, to induce a detectable signal the analyte must have significant mass. Thus glycans are typically immobilized on the gold surface (often using neoglycoproteins,[30] i.e. glycans synthetically coupled to a protein backbone), and the more substantial lectins are used as the binding analytes. This can bias the analysis of single lectin−glycan interactions as presentation and density of the glycan is a critical parameter in CRD binding, and the immobilization methodology can alter this.[31] Though more difficult, lectins can also be immobilized on the SPR surface and detect glycosylated analytes, but again these must have enough mass to transduce a change in refractive index.

We show that the SWNT-based fluorescence sensors developed in this work demonstrate loading curve signals competitive with SPR, in both shape and analysis technique, but they differ in a few significant ways. First, the detection scheme is reversed. The lectins are the tethered sensors, and the glycans are the analyte in solution. This allows us to determine the kinetics of free glycans as well as glycoproteins giving us precise control over carbohydrate presentation in the interaction. Second, the amount of analyte needed for each experiment (2 μg of glycosylated protein or 100 ng of free glycan) is smaller than what is necessary for SPR experiments, which require analyte flow to overcome mass-transport effects (at its best, SPR requires 20−250 μg of analyte protein[32]). Third, each SWNT-sensor spot can be tethered to different lectins and illuminated simultaneously, creating the potential for a multiplexed, quantitative detection of analyte binding analogous to an array-reading SPR machine with distinct advantages in sample size and run time.

2. EXPERIMENTAL SECTION

2.1. Lectin Expression. The resulting plasmid pET41GafD and pET41-PAIIL were transformed into BL21(DE3) Star (Invitrogen) according to standard procedures.[33] A single colony was used to inoculate 5 mL of LB medium containing kanamycin (50 μg mL^{-1}). 3 mL of the overnight culture at 37 °C were used as an inoculum to a 350 mL flask of LB containing 50 μg mL^{-1}, and this was incubated again with shaking at 37 °C. Heterologous protein was induced by the addition of isopropyl β-D-1-thiogalactopyranoside (IPTG, final concentration 1 mM) once this culture had reached log phase (A_{600} of 0.6). Growth was continued for 6 h before the cells were harvested by centrifugation. For His-tag protein purification, a harvested cell pellet was washed twice with phosphate-buffered saline, PBS (10 mM, pH 7.4), and then lysed with Complete Lysis-B (Roche Applied Science). The crude lysate was clarified by centrifugation prior to application to a 3 mL Ni-NTA agarose column (Qiagen). Nonspecifically bound proteins were removed from the column with wash buffer (50 mM NaH_2PO_4, pH 8.0, 300 mM NaCl, 20 mM imidazole), and bound His-tag GafD and PAIIL were eluted with elution buffer (50 mM NaH_2PO_4, pH 8.0, 300 mM NaCl and 250 mM imidazole). Eluted samples were analyzed by 15% SDS-PAGE, and the protein concentration was determined with a BCA assay kit according to manufacturer's instructions (Pierce). To change the buffer with PBS (10 mM, pH 7.4), the eluted solution was centrifuged through a centrifugal filter with a molecular cutoff of 10 kDa (Millipore), and the concentration of lectin was finally adjusted to 4 mg mL^{-1}.

2.2. Glycan and Model Glycoprotein Probes. Biotinylated glycans were provided by the Consortium of Functional Glycomics − Scripps Institute Group. For this work, glycans B121 (GlcNAcβ-SpNH-LC-LC-Biotin) and B158 were used (Fucα1-2Galβ1-4Glcβ-SpNH-LC-LC-Biotin) where Sp is 2-azidoethyl and LC-LC biotin is a standard biotin reagent with an extra-long spacer group (Pierce ID# 21343). The lyophilized sugars were dissolved in 3 mL of 1× PBS to create stock solutions and stored at −20 °C. To construct model glycoprotein probes, the biotinylated glycans were incubated with streptavidin (Sigma Aldrich SO677) for 1 h at 20 °C in a 6:1 molar ratio to allow maximum binding to the four biotin binding sites on each streptavidin. Excess biotinylated glycans were filtered away from the glycoproteins by centrifugation through an Amicon filter (16 300*g* on Labnet Inc. centrifuge, 10 min, 30 000 kDa cutoff, Milipore). The glycoproteins were washed on the filter 3× (400 μL PBS) and then resuspended in PBS at the desired concentrations.

2.3. Native PAGE Binding Analysis. The interaction between lectin and glycan was analyzed by 15% native PAGE according to the method of Schägger and von Jagow with minor modifications.[34] Briefly, electrophoresis was performed using a Mini Protean Electrophoresis system (Bio-Rad, USA) under nondenaturing conditions to examine molecular interactions. Nonreduced protein/glycan samples (GafD Lectin held constant at 30 μg per lane, GlcNAc-Strept added at 5, 10, 20, and 30 μg) in the sample buffer (20% glycerol, 200 mM Tris-HCl, pH 6.8, 0.05% bromophenol blue) were applied to the gel (gel buffer: 25 mM Tris-HCl, 200 mM glycine). Electrophoresis was performed at 80 V for 120 min. After electrophoresis, the protein bands were visualized by staining with Coomassie Brilliant Blue R-250.

2.4. Construction of Chitosan-SWNT Sensor Chips. To increase the reproducibility of our sensors, we have introduced a careful automated printing method of the chitosan gel (Supporting Figure 1). Patterned glass microscope slides (Tekdon) were inserted in a microarray printer (Digilab MicroSys System) where the robotic head was

Scheme 1. Processing Steps To Tether a His Tag Sensor Protein to SWNT[a]

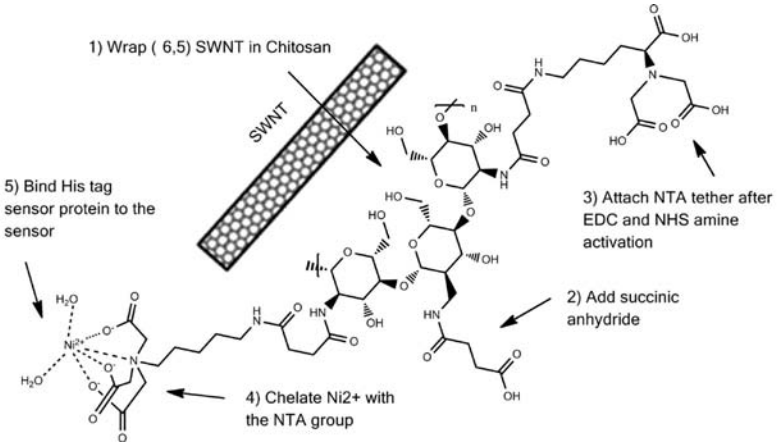

[a] (1) Wrap SWNT in chitosan, (2) functionalize chitosan with carboxylic acids, (3) attach tethered NTA group, (4) chelate nickel with NTA, (5) add His tag sensor protein to SWNT.

programmed to dispense alternating layers of chitosan-SWNT (0.25 wt % chitosan (CHI), 1 vol% acetic acid, 30 μg/mL suspended (6,5) SWNT) and cross-linker (10 vol% glutaraldehyde). The suspended SWNT was made from Southwest Nanotechnologies, Inc. CoMoCAT nanotubes sonicated in 0.25 wt % chitosan (CHI) and 1 vol% acetic acid for 45 min at 40% amplitude with a probe−tip sonicator (Cole Parmer, Model CV18). For each sensor spot 10 alternating layers of SWNT-CHI and cross-linker were printed at 100 nL per layer, resulting in a highly uniform gel of 1 μL of SWNT-CHI material. The chips were printed in a humidified enclosure (85% RH) at 25 °C and allowed to cross-link overnight in the same environment. Nickel-NTA groups were introduced as previously reported.[15] Briefly, the chips were washed with a dilute basic buffer (0.01 M NaOH) and water three times. Carboxylic acid groups were introduced to the chitosan wrapped SWNT by bathing the chips in succinic anhydride (0.1 M) overnight (Scheme 1, step 2).

The chips were then washed three times with water, and the carboxylic acid groups were activated via *N*-(3- dimethylaminopropyl)-*N*′-ethyl-carbodiimide hydrochloride (EDC, 0.1 M) and *N*-hydroxysuccinimide (NHS, 0.1 M). The chips were bathed in this solution for 2 h at 25 °C and examined for the expected formation of bubbles. The chips were again washed and allowed to bathe in a solution of a linked tricarboxylic acid group (*Nα*,*Nα*-bis(carboxymethyl)-L-lysine aka NTA, 33 mM) overnight (Scheme 1, step 3). The chips were washed in water again and stored in a 100 mM solution of $NiSO_4$ to allow maximum binding of nickel to the NTA chelating groups (Scheme 1, step 4). Thus in each experiment the SWNT sensors start in their maximally quenched state due to the close proximity of the nickel. During experimentation the excess $NiSO_4$ is washed away with water and the sensor protein, His-tagged lectin, is tethered to the SWNT sensors via the chelated nickel group (Scheme 1, step 5). The large protein groups cause the nickel group to move away from the SWNT sensor, due to steric loading (discussed below), and part of the quenched fluorescent signal returns.

2.5. Ensemble Measurements of Sensors. A custom-made near-infrared inverted microscope (Zeiss D.1 Observer) setup allows us to probe the fluorescent emissions of our SWNT sensors (Figure 1a). The chips are secured on the microscope stage, and the objective (50×/0.7 Zeiss) is pushed into contact with a blank portion of the glass slide (no SWNT-CHI) to obtain a 5 s background spectrum, which is subsequently subtracted from the response spectra. The objective is then moved under an SWNT-CHI gel spot and again pushed in contact with the glass slide. By placing the objective in the maximum *z*-axis position, the microscope can image a higher plane of the SWNT-CHI gel where more analyte response is observed. The SWNTs are excited by a 785 nm laser (B&W Tek, 495 mW), and the emission is sent to a spectrometer (Princeton Instruments Acton SpectraPro 2500i Spectrograph) and accompanying nIR camera (Intervac MOSIR Camera 350). The spectra are collected via WinSpec software (Princeton Instruments) and analyzed with custom Matlab (Mathworks) code. To maximize signal stability, the spectrometer is cooled with liquid nitrogen 2 h prior to experimentation and the laser is allowed to reach peak stability for 2 h. The SWNT-CHI gel has a small transient region when first exposed to the laser due to local heating and further permeation of Ni^{2+} in the gel; thus each spot is pre-exposed to the laser for 5 min before data are gathered. Data are gathered in the form of emission intensity spectra (950−1250 nm) integrated for 5 s.

A typical experiment was run for approximately 1000 frames (at 5 s each) and included a few addition and washing steps to detect lectin−glycan binding (Figure 1b). First $NiSO_4$ was again added to ensure that the SWNT sensors were responsive and that the NTA chelating groups were fully loaded with Ni^{2+} groups. The nickel was then washed away with PBS three times, leaving ∼20 μL of PBS on the sensors. The His-tag lectin was then added to the sensor (20 μL at 2 mg/mL) and allowed to bind for 300 s. Excess lectin was again washed by PBS three times, and 20 ± 1 μL PBS were left to bathe the sensor. The sensor was allowed to equilibrate for 100 s, and 20 μL of analyte were added. The analytes tested in this paper include free biotinylated glycans, glycans tethered to streptavidin, and anti His-tag antibody. Each of these, upon binding, causes an increase in SWNT luminescence (Figure 1b). The sensor response was recorded for 500 s. It is essential to record stabilization frames before and after the analyte addition in order to correct for any focal drift caused by the tension of the objective in contact with the glass slide (see Results section).

2.6. Single SWNT Sensor Measurements. A second custom microscope was used to collect emission intensities of single SWNT sensors. The SWNT-CHI gel was diluted to 3 μg/mL of SWNT and spin-coated (3000 rpm for 30 s on Laurell Technologies Corporation, WS-650MZ-23NPP/LITE) on glass-bottom Petri dishes (MarTec Corp). The Petri dishes were then placed on the microscope platform (Zeiss D.1 Observer), and the oil-immersed objective (Zeiss 100×/1.46) was focused on the SWNT sensors on the glass surface. The SWNTs were excited by a 660 nm laser (Crystal Laser, 100 mW), and the emission intensities were recorded by a nitrogen-cooled InGaAs array (Princeton Instruments). Again WinSpec software (Princeton Intrsuments) was used to collect the data in the form of a stacked Tiff

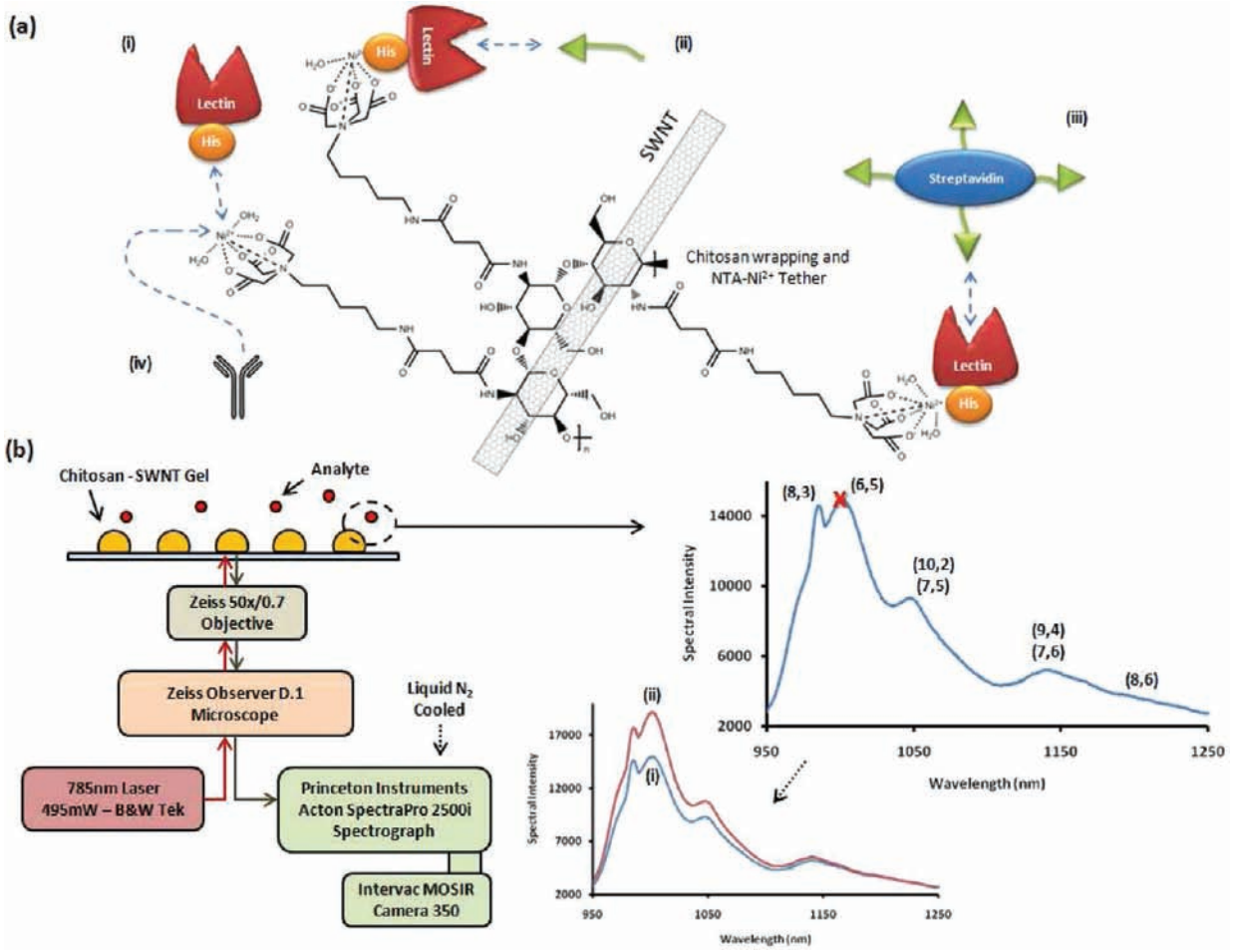

Figure 1. Ensemble measurements of Chitosan-SWNT sensors for glycan lectin detection. (A) The chistosan wrapped SWNT sensors are processed (see text) to include tethered NTA groups and chelated Ni^{2+} so that His-tagged lectins (i) can attach to the sensors. An analyte (anti His-tag antibody (iv), free biotinylated glycan (ii), or glycan tethered to streptavidin (iii)) is added, and the emission fluorescence is increased (Part B (i) to (ii)) due to the Ni^{2+} group moving away from the SWNT, caused by steric loading of the sensor (see text). (B) Ensemble measurement setup: the chitosan-SWNT gel is spotted onto glass chips which are excited by a 785 nm laser in a custom inverted microscope setup. The resulting emission spectra are then analyzed looking at the intensity of the (6,5) nanotube peak over time.

image where pixel values corresponded to spectral intensity. These Tiff images were then analyzed using custom Matlab code (Mathworks) to (1) construct an intensity versus time trace for each SWNT sensor, (2) noise reduce the intensity signal, (3) fit the signal to a stepwise curve, and (4) determine the kinetic rates for each SWNT sensor according to a previously published model.[35,36]

3. RESULTS AND DISCUSSION

We first confirmed that our Streptavidin-based model glycoproteins bind to our expressed His-tag lectins using native PAGE gel analysis, which allows the protein−protein complex to remain in its native, nondenatured form. Note that separation is dictated by native complex charge and morphology, not strictly molecular weight as in SDS-PAGE.[37] The resulting gel (Figure 2) clearly indicates a bound complex that arises when the GlcNAc-streptavidin probe (1 mg/mL) is added in solution with GafD lectin, a lectin from *Escherichia coli*, which binds β-GlcNAc (3 mg/mL).

Next the time response of the sensor during construction and various analyte additions was analyzed using the ensemble measurement technique outlined in Figure 1. In the first test, Ni^{2+} was added (100 mM) which caused a clear quenching

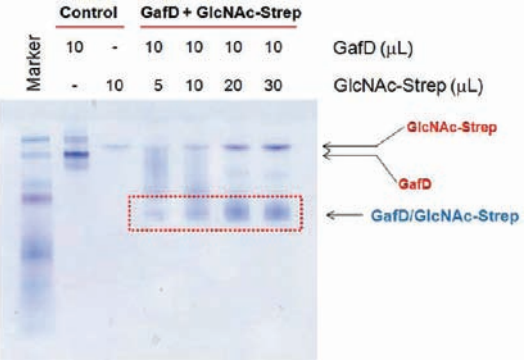

Figure 2. Native PAGE gel of GlcNAc-Streptavidin (1 mg/mL) to GafD Lectin (3 mg/mL) in solution. The gel reveals an increasing band of GafD−GlcNAc conjugate as more GlcNAc-Streptavidin is added to solution.

response as the Ni^{2+} interacted with the exposed SWNTs decreasing their fluorescence (Figure 3a). The effect of divalent cation quenching of nanotubes is established in the literature.[38,39]

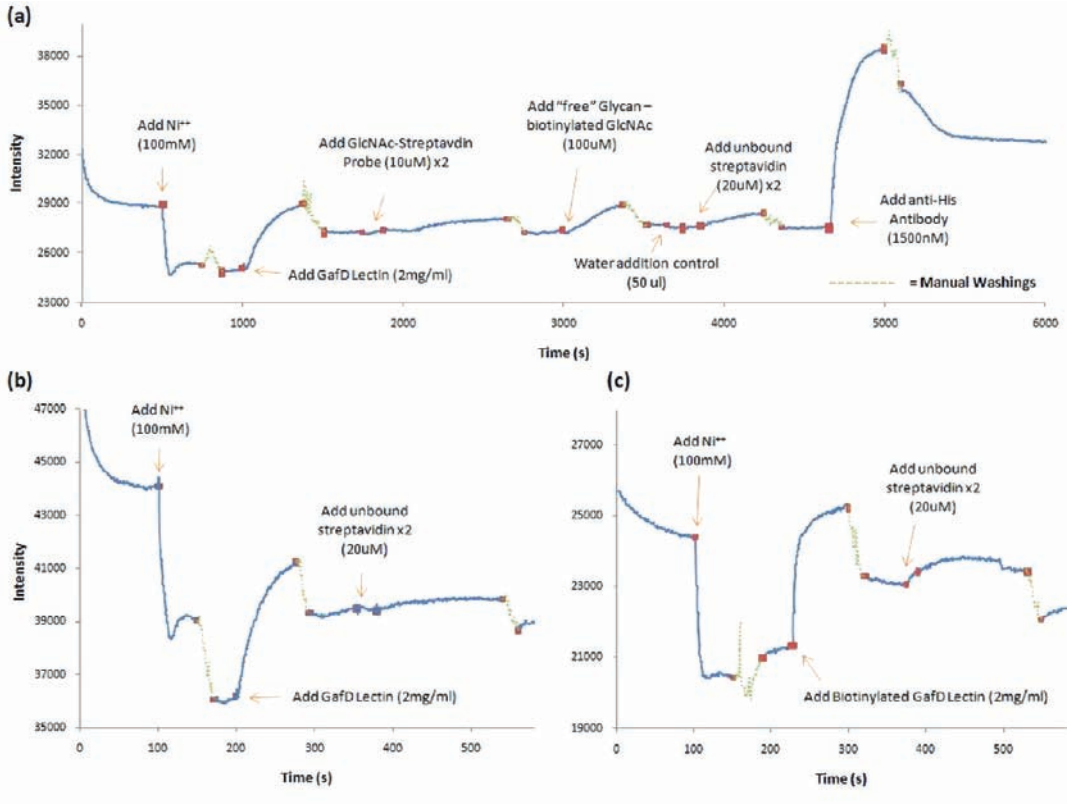

Figure 3. Time response curves of sensor chemistry steps and analyte additions. (A) Responses during construction of a GafD lectin sensor and responses to free GlcNAc, GlcNAc-Streptavidin, unconjugated streptavidin, and anti His-tag antibody. Each of the additions with known affinity exhibit a loading similar to those found in SPR experiments. (B) Negative control: adding unconjugated streptavidin to GafD lectin results in negligible response. (C) Positive control: adding unconjugated streptavidin to biotinylated GafD lectin.

In brief, the SWNT exciton formed by laser excitation is affected by the electronic field of the metal ion and caused to decay in nonradiative pathways; thus the fluorescent emission of the SWNT is effectively reduced as the metal ion comes in close proximity. The excess Ni^{2+} was then washed away, and the His-tagged lectin GafD was added (40 μg in 20 μL). A loading curve (much like that observed in SPR assays) was observed as the lectin binds to the NTA–Ni^{2+} complexes. The mechanism, consistent with our previous analysis, is that the increase in SWNT fluorescence is caused by an increase in the distance between the Ni^{2+} complex, lessening its proximity quenching effect.[15] Both steric loading and multivalent effects can influence this as discussed below. The excess lectin is removed and the Streptavidin-GlcNAc probe is added (40 μg in 40 μL), in two steps. Again, an SPR-like loading curve is observed, except with slower kinetics and less overall response. The excess Streptavidin-GlcNAc probe is washed away, and free biotinylated GlcNAc is added (20 μL of 100 μM). Again the loading curve is observed. After washing away the excess free glycan, we added 40 μL of PBS to the system to ensure that the loading responses were due to the analyte and not some focal change due to increased mass on the sensor. We then checked to see if the biotinylated glycans, now bound to the sensor, were accessible to blank streptavidin. Upon streptavidin addition we see another loading curve, with slower kinetics, confirming binding of streptavidin to the biotin ends of glycans decorated on the SWNT-Lectin sensors. As a positive control, we used an anti His-tag antibody, as previously[15] to verify the integrity of His-tag binding at the end of the experiment. Here, binding to the His-tagged lectin displaces it and increases the distance between the SWNT and Ni^{2+}, causing the reported increase.

Two other time-series analyses were conducted as a negative and positive control. In the negative control, blank streptavidin was added to the sensor, after Ni^{2+} and GafD lectin loading (Figure 3b). No loading curve is observed. In the positive control blank streptavidin is again used as the analyte, but this time the GafD lectin is biotinylated (Pierce Kit 21455). Upon addition of streptavidin we see the expected loading curve (Figure 3c).

The time-series analyses reveal activation limited kinetic responses as expected for our free glycan and streptavidin-tethered probes, since the response rates are highly dependent upon the analyte and therefore not limited by diffusion through the chitosan matrix. To obtain forward and reverse kinetic rates of binding we analyzed the loading curves of the sensors at varying analyte concentrations. Assuming our reaction model is that of a single-site surface absorption,

$$G + L \leftrightarrow GL \tag{1}$$

where G is the glycosylated analyte, L is the lectin binding sites, and GL is the bound complex; then we would expect the following kinetic model to express the rate of change of bound complex:

$$\frac{d[GL]}{dt} = k_f[G][L] - k_r[GL] \tag{2}$$

dx.doi.org/10.1021/ja2074938 |J. Am. Chem. Soc. 2011, 133, 17923–17933

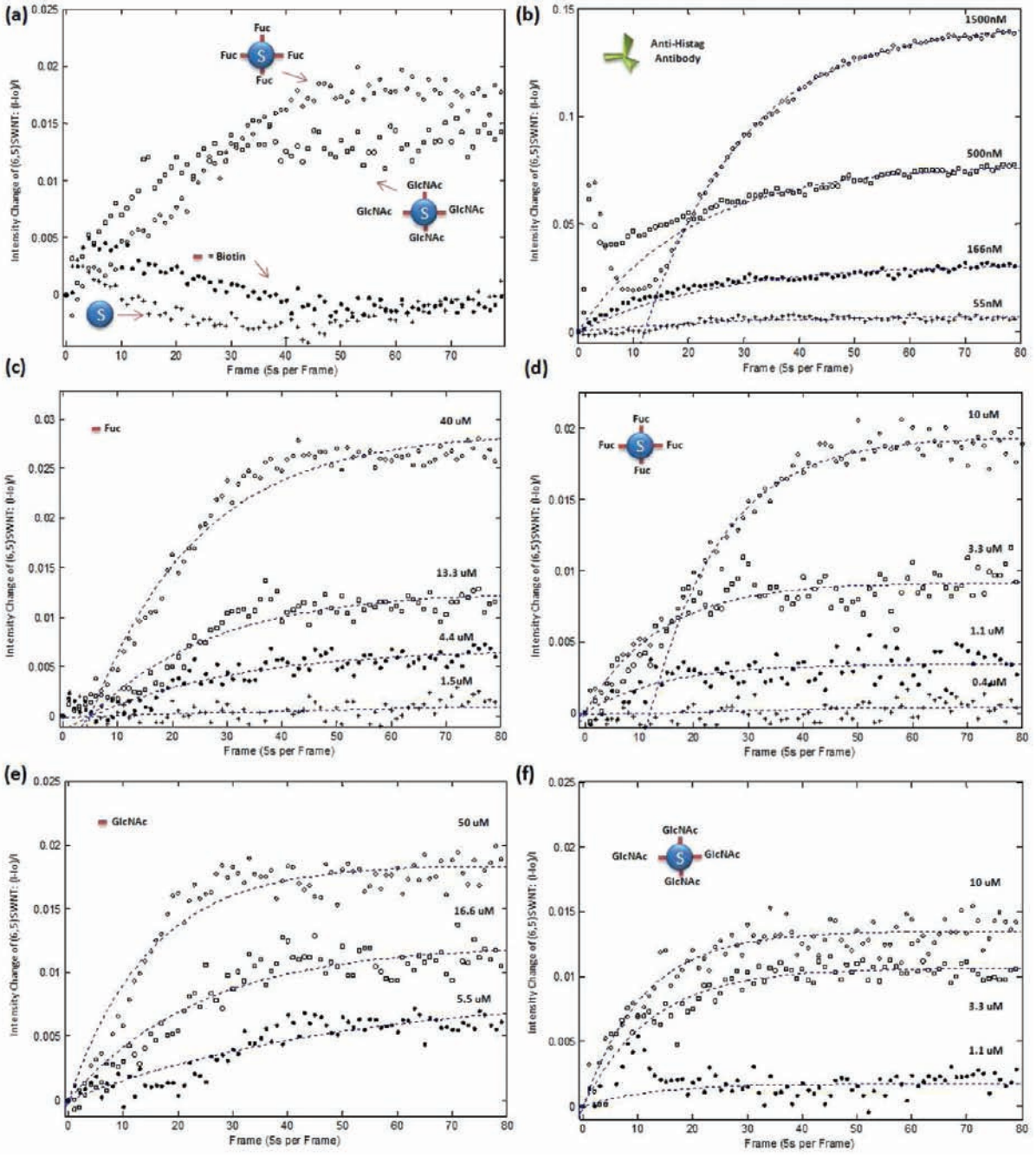

Figure 4. Concentration dependent loading curves of various analytes to SWNT-Chitosan sensors. (A) Control curves showing positive response of GlcNAc-Strept to GafD and Fuc-Strept to PA-IIL and negative responses to biotin and blank streptavidin. Concentration dependent loading curves for (b) anti His-tag antibody to GafD lectin, (c) biotinylated Fuc to PA-IIL, (d) Fuc-Streptavidin to PA-IIL, (e) biotinylated GlcNAc to GafD, and (f) GlcNAc-Streptavidin to GafD. The dotted lines denote the kinetic model fit, and resulting parameters are reported in Table 1.

The concentration of the free Lectin sites at a given time can be expressed as

$$[\mathrm{L}]_t = [\mathrm{L}]_{to} - [\mathrm{GL}]_t \quad (3)$$

Thus eq 2 can be rewritten as

$$\frac{d[\mathrm{GL}]}{dt} = k_f[\mathrm{G}]([\mathrm{L}]_{to} - [\mathrm{GL}]_t) - k_r[\mathrm{GL}] \quad (4)$$

We assume that the analyte concentration, [G], is constant (as the bulk of fluid above the sensor is large in comparison to the number of lectin binding sites). The change in our fluorescent intensity (I) is a measure of the change in bound complex [GL], so an analogous form of eq 4 for our sensor system would be

$$\frac{dI}{dt} = k_f C_g(I_{max} - I_t) - k_r(I_t) \quad (5)$$

This equation can be rearranged as to lump the kinetic parameters together into one kinetic variable (k_s) as is done in fitting

Table 1. Kinetic Parameters Found from Concentration Dependent Curves[a]

Experiment	R^2 Val	K_f $(\mu M \cdot s)^{-1}$	k_r (s^{-1})	K_D (μM)	95% Confidence K_D (μM) Range
ATB to GafD	0.9707	2.00×10^{-6}	0.0082	4	2−14
Fuc-Biotin to PA-IIL	0.8649	7.00×10^{-5}	0.0074	106	58−192
Fuc-Strept to PA-IIL	0.9367	0.0001	0.0142	142	N/A
GlcNAc-Biotin to GafD	0.941	0.0002	0.0037	19	11.5−25.5
GlcNAc-Strept to GafD	0.99	0.0003	0.015	50	N/A

[a] 95% confidence ranges are not available for the less-affined glycan-streptavidin probes with the current platform.

SPR data:[40]

$$\frac{dI}{dt} = k_f C_g I_{max} - k_s(I_t) \quad (6)$$

$$k_s = k_f C_g + k_r \quad (7)$$

Integrating eq 6 yields the equation for the absorption curve:

$$I_t = M(1 - e^{-k_s t}) + I_o \quad (8)$$

$$M = \frac{k_f C_g I_m}{k_f C_g + k_d} \quad (9)$$

Thus by obtaining absorption curves at three to four different concentrations of glycosylated analytes (C_g) and fitting them to eq 8, one can plot k_s versus C_g. A linear trend supports this binding mechanism and kinetics. As eq 7 shows, the slope and y-intercept of this line correspond to k_f and k_r respectively.

Concentration dependent absorption curves were obtained for controls, anti His-tag antibody, free biotinylated glycans (Fuc and GlcNAc), and glycans tethered to streptavidin (Fuc and GlcNAc). The controls (Figure 4a) revealed a positive response for the Fuc-Streptavidin probe to PA-IIL lectin and GlcNAc-Streptavidin probe to GafD lectin. It is also revealed a negligible response to blank streptavidin as well as biotin. Here we must mention that the first 20 frames of the absorption curve often contain artifacts due to the manual additions of analyte (pipet tip to edge of spot). Thus in fitting the absorption curves to eq 8 we have set the fit parameters to optimize the fit on the curved portion of the isotherm rather than the artifacts at the beginning of the curve. Also the absorption curves have been linearly corrected for focus drift caused by tension on the z-axis focus due to direct contact with the glass. This small correction (less than 0.05% of the signal) is made by linearly fitting the end of the absorption curve when the system is again at equilibrium.

The curves for anti His-tag antibody (Figure 4b) were obtained for 1500, 500, 166, and 55 nM concentrations interacting with GafD lectin tethered to the SWNT sensor. The resulting k_s fit was highly linear ($R^2 = 0.971$), and the resulting k_f, k_r, and K_D values are tabulated in Table 1. The K_D of 4 μM found for our murine produced anti His-tag antibody (Sigma H1029) correlates well with the 1 μM found by Biacore SPR studies.[41] The concentration dependent curves for free biotinylated fucose (40, 13.3, 4.4, and 1.5 μM) to PA-IIL lectin (Figure 4c) and tethered fucose-streptavidin probes (10, 3.3, 1.1, and 0.4 μM) to PA-IIL lectin (Figure 4d) also fit the SPR-like kinetic model well, and their kinetic parameters are reported in Table 1. The K_D values of 106 and 142 μM found by our sensor for free and tethered fucose to PA-IIL are weaker than the previously reported 3 μM found by isothermal titration microcalorimetry (ITC).[42] It is often observed that surface tethering of a receptor results in an increase in K_D, often by orders of magnitude;[43] therefore the decreased affinity of our surface tethered approach compared with ITC measurements of solution phase binding is expected. The discrepancy in K_D measurement may also arise in the chemical modification of the glycan or the tethered presentation of the lectin on the surface. The binding of free biotinylated GlcNAc (50, 16.6, and 5.5 μM) and GlcNAc-streptavidin probe (10, 3.3, 1.1 μM) to GafD lectin (Figure 4e−f) also followed the model. The fitted kinetic parameters are reported in Table 1. To our knowledge, this is the first measurement of GlcNAc to GafD kinetics on any platform, although there are many glycan-array studies showing a high relative affinity of GlcNAc to GafD over other glycans.[44−47]

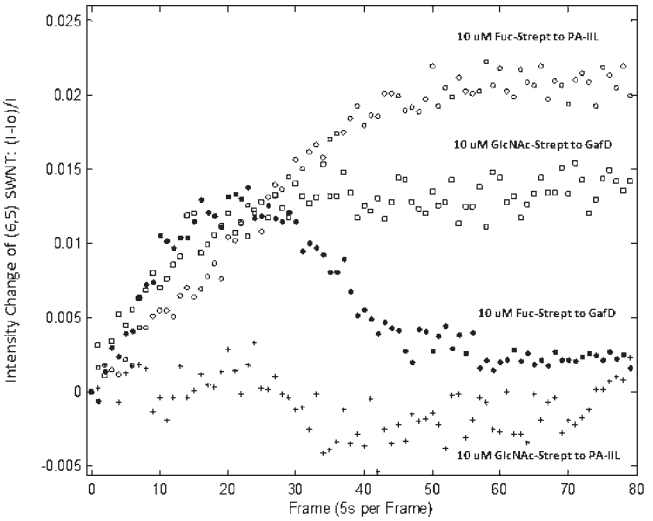

Figure 5. Selectivity of SWNT-Lectin sensors. Greater response of known high affinity pairs (Fuc to PA-IIL and GlcNAc to GafD) than the cross reactions.

We also checked the selectivity of the SWNT-Lectin sensors by measuring the cross response of our glycans and lectins (Figure 5). The PA-IIL lectin showed negligible binding to the GlcNAc-Streptavidin probe, whereas the GafD lectin exhibited a small affinity for Fuc-Streptavidin. However the cross affinity of Fuc-Streptavidin to GafD was much smaller than the known strong-binding combination of fucose to PA-IIL. This demonstrates that the SWNT-lectin sensors could potentially be used to distinguish between sugar groups, especially as the sensor signal is optimized.

The overall change in signal intensity is small (3−5%) for ensemble measurements of glycan−lectin binding for this system (Figure 3). We asked if the observed response was homogeneous, meaning that each SWNT responds to this small degree, or inhomogeneous, where a subset of SWNTs modulate to a much greater extent. The use of single nanotube spectroscopy allows one to address this question (Figure 6a). Our laboratory has used this approach for other single molecule sensitive platforms using SWNT-based sensors for H_2O_2,[48,49] NO,[35,50] glucose,[43] and

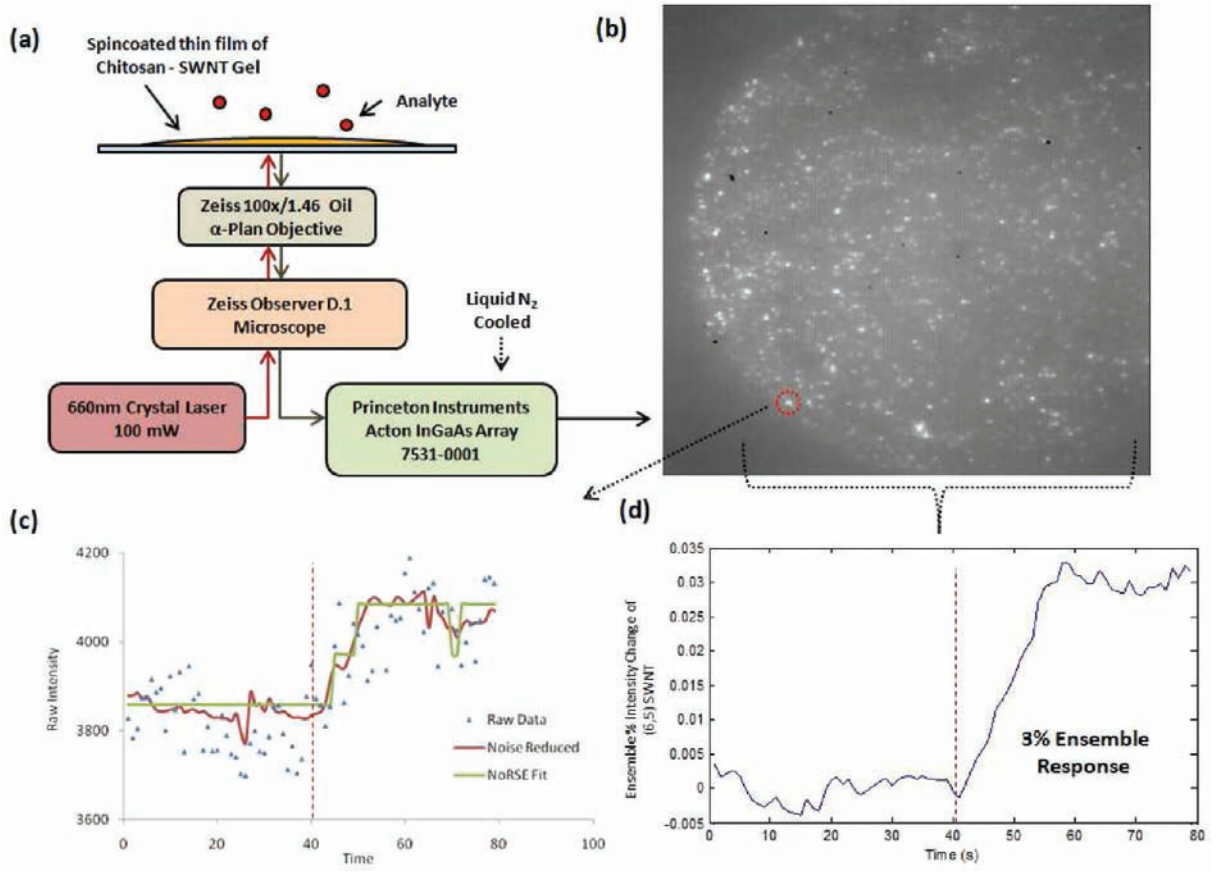

Figure 6. Single SWNT sensor measurements. (A) Experimental setup: a thin film of chitosan-SWNT is spin-coated on the glass chip and excited by a 660 nm crystal laser, and the resulting emission is analyzed by an InGaAs array. (B) The array produces a tiff image per time frame where each pixel value denotes the fluorescent intensity; in this manner single SWNT can be visualized. (C) By binning 2 × 2 pixel regions for the brightest 1000 SWNT, individual traces of fluoresce intensity versus time can be created for each SWNT sensor. These traces are then noise-reduced and fitted to determine kinetic parameters (--- denotes addition of GlcNAc-Streptavidin at 10 μM to GafD). (D) An ensemble average of the individual SWNT sensors can be approximated by adding the signals of 150 SWNT sensors (--- denotes addition of GlcNAc-Streptavidin at 10 μM to GafD).

nitroaromatics.[51] The resulting thin film of chitosan wrapped SWNTs (Figure 6b) was imaged at a frequency of 1 frame per second using our InGaAs array setup. Using software developed in house, we can analyze the movies of SWNT fluorescence and extract intensity time traces for each of the individual SWNT sensors (Figure 6c).[36] We have also recently developed an efficient algorithm (submitted work to *Bioinformatics*; annotated code is freely available online at http://web.mit.edu/stranogroup/NoRSE.txt) for fitting large quantities of these time traces to embedded fluorescent levels.[52] Briefly, the algorithm uses an optimized form of an established noise-reduction algorithm for biological experiments[53] to clean the traces (Figure 6c). It then evaluates all-points histograms of each trace to determine the unique fluorescent states of each trace. The resulting step traces (Figure 6c) are then used to determine the forward and reverse kinetics of each SWNT sensor. Before analyzing the kinetics of each individual trace, the prior ensemble experiments were approximated by summing the intensity values of noise-reduced traces from 150 individual SWNT sensors (Figure 6d). The resulting signal modulation of the GlcNAc-Streptavidin probe (10 μM) to GafD is nearly identical to that of our ensemble measurements (~3.5% response).

The kinetic analysis of individual SWNT sensors helps determine the locations of "strong transducers" based on overall signal modulation and dissociation constant. Intensity versus time traces are extracted from the brightest 1000 SWNT sensors (Figure 7a) and analyzed for a time period of 40 s before and after glycan addition. The location of the eight top SWNT sensors based on signal modulation (each greater than 5%) is easily determined (Figure 7b). To determine the K_D of each SWNT sensor, the traces are noise-reduced and fitted by the NoRSE algorithm[52] and then kinetic parameters are found with the previously reported Birth−Death kinetic model.[35,36] The first 40 s of the trace (before glycan addition) are used to determine the background k_f and k_r rates for each SWNT sensor (due to intrinsic fluctuations of the tethered group) and then subtracted from the k_f and k_r rates found after glycan addition. Of the 1000 traces analyzed, 289 traces had sufficient signal over the background fluctuations to determine the K_D upon glycan addition (Figure 7c). Locations of the four strongest transducers, with K_D values less than 10 μM, were determined. It is interesting that these strong kinetic transducers were not the brightest SWNT traces but rather traces with 50 to 75% the intensity of the brightest recorded. This may reflect the insensitivity of small SWNT bundles to this sensing mechanism. Bundles appear brighter as a composite fluorescent spot, and their construction would necessarily shield the interior SWNT from modulation. Future work will explore this. The population of 289 SWNT

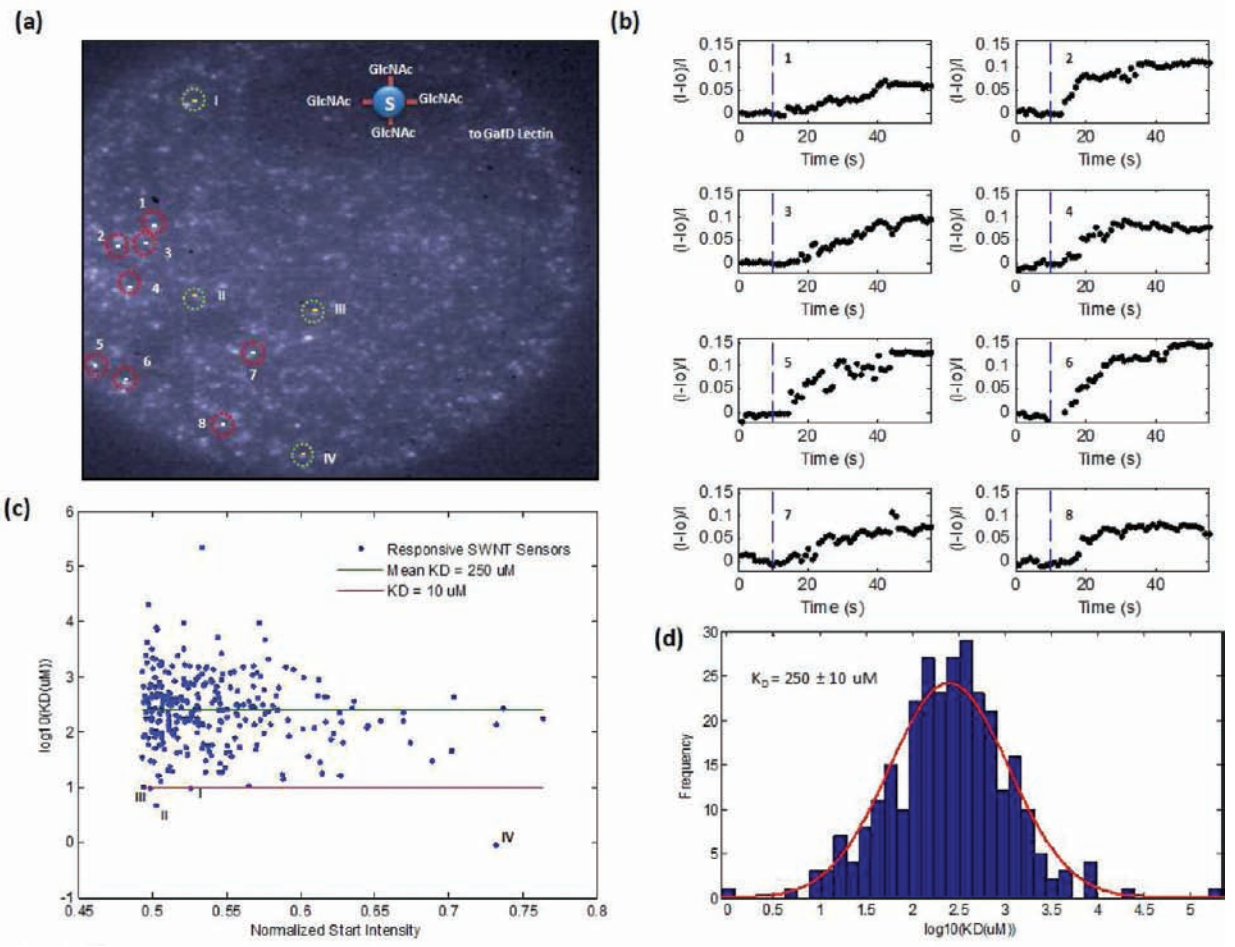

Figure 7. Single SWNT sensor measurement results. (A) a thin film of CHI-SWNT is imaged by the single sensor setup showing a field of sensors on the glass surface. (B) The sensors can be evaluated individually to find which ones give maximum signal modulation. Shown are curves from eight of the most responsive with their positions marked by red circles in (A). Vertical dashed lines denote the time of analyte addition. (C) 289 SWNT sensors have signals strong enough to determine K_D values; these are plotted versus starting intensity. Four sensors are found to have strong K_D values (<10 μM), and their locations are denoted by green circles on (A). (D) The population of K_D values yields a single Gaussian distribution when plotted as a histogram of $\log_{10}(K_D)$ values with a mean K_D of 250 μM.

transducers was analyzed to find a K_D of 250 ± 10 μM (Figure 7d). Further optimization of glycan−lectin kinetic parameters from single molecule analysis could be achieved with a system that has a faster sampling time than the current limit of 1 frame per second.

The SWNTs may differ in their ability to report the Glycan−Lectin binding events due to accessibility to the analyte in the gel, inhomogeneous chemistry modifications (more or less NTA groups per SWNT), SWNT defects, and the influence of multivalent binding. We note that we do not see single molecule steps associated with discrete adsorption steps, as we have seen for other, small molecule quenchers.[35,51] In this case, the interaction of the analyte with the SWNT is indirect, through the spacer chemistry that adjusts the Ni^{2+} distance to the SWNT. This mechanism need not be discretized as in the case of adsorption/desorption of a molecular quencher directly on the SWNT surface. In the glycan/lectin system, the quenching distance is continuous. Nevertheless, single SWNTs do respond and contribute to the ensemble response. The fact that the response can be monitored in a single 2 × 2 pixel spot offers possibilities to dramatically decrease the quantity of the required analyte. Even the current responses are an improvement over SPR (which can require 20−250 μg of protein analyte at optimal run conditions[32]) since we utilized less than 2 μg of glycosylated protein or 100 ng of free glycan as the analyte probe. The amount of lectin (20 μg) used for the SWNT sensors can also be dramatically reduced be microprinting smaller volumes of protein directly on an array of optimally responding SWNT sensors.

Finally, these data sets reveal more about the response mechanism of our Ni-NTA tethered SWNT sensor. As demonstrated previously,[15] the Ni^{2+} appears to act as a proximity quencher[38] to the SWNT; however in this work we have now done careful time-series analyses rather than static before and after measurements. In each case of analyte binding, the fluorescent signal increases consistent with the Ni^{2+} group moving further away from the SWNT group. According to this model, the higher the affinity an analyte has for the sensor protein, the larger the observed increase. To demonstrate this, we include another time trace of the anti His-tag antibody response to GafD (Figure 8) which includes an addition step of adding imidazole (250 mM). Imidazole exhibits a higher affinity for Ni^{2+} than a His-tag group and is often used in protein purification to elute proteins bound in a Ni-agarose column. The time trace shows

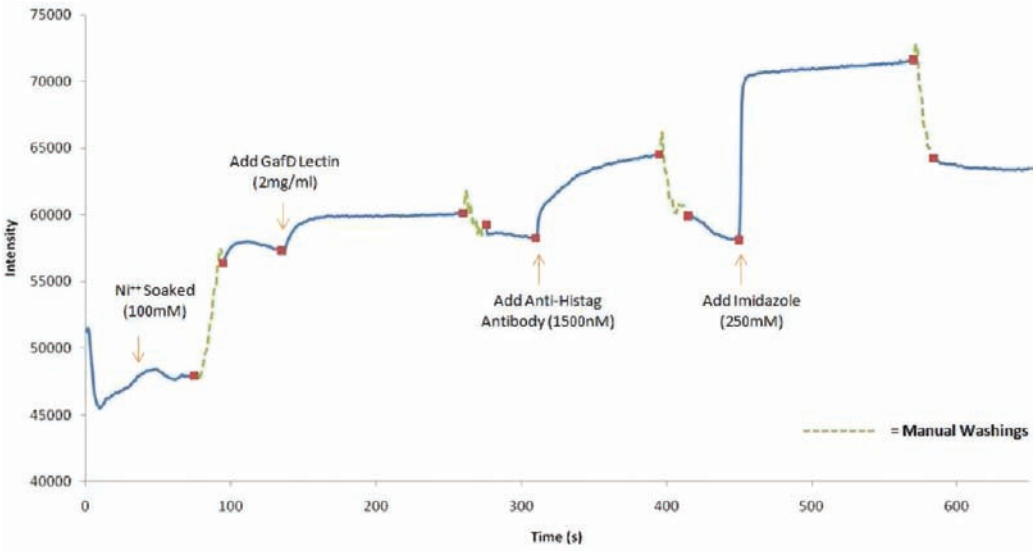

Figure 8. Time response curve showing increased fluorescence response upon addition of all affined analytes, including Imidazole. Upon addition, the analytes cause steric loading of the tether causing the Ni^{2+} to move away from the SWNT; this causes a partial return of the quenched SWNT fluorescence.

that for each of the additions (His-tag lectin, antibody, and imidazole) we see an increase in SWNT intensity. This seems to suggest that the increase in tether length is due to "steric loading" of the NTA−Ni^{2+}−sensor protein complex. As more analyte binds to the complex, the required space increases and the tethered group's fluctuations tend to be further from the nanotube. Multivalency of the analyte may also play a role (as in the case of glycan-streptavidin addition) as multiple NTA−Ni^{2+}−sensor protein complexes stretch to meet a single, multivalent analyte.

4. CONCLUSIONS

In conclusion, we demonstrate a sensor array for measurement of binding kinetics of model glycans. The approach uses recombinant lectins as glycan recognition sites tethered via Histidine tags to Ni^{2+} complexes that act as fluorescent quenchers for semiconducting single-walled carbon nanotubes embedded in a chitosan hydrogel spot. As model glycans, both free and streptavidin-tethered biotinylated monosaccharides are studied with two higher-affined glycan−lectin pairs: fucose (Fuc) to PA-IIL and *N*-acetylglucosamine (GlcNAc) to GafD. We find that the dissociation constants (K_D) for these pairs as free glycans can be measured as 106 and 19 μM respectively and streptavidin-tethered 142 and 50 μM respectively. The absolute detection limit for the current platform was found to be 2 μg of glycosylated protein or 100 ng of free glycan to 20 μg of lectin. Glycan detection (GlcNAc-streptavidin at 10 μM) is demonstrated at the single nanotube level as well by monitoring the fluorescence from individual SWNT sensors tethered to GafD lectin. Over a population of 1000 nanotubes, 289 of the SWNT sensors had signals strong enough to yield kinetic information (K_D of 250 ± 10 μM). This single molecule approach allows us to identify the locations of "strong transducers" on the basis of kinetic strength (four sensors with K_D < 10 μM) or overall signal modulation (eight sensors with >5% quench response). The brightest SWNTs are clearly not the best transducers of glycan binding. SWNTs ranging in intensity between 50 and 75% of the maximum show the greatest response. The ability to pinpoint strong-binding, single sensors is promising to build a nanoarray of glycan−lectin transducers as a high throughput method to profile glycans without protein labeling or glycan liberation pretreatment steps.

■ ASSOCIATED CONTENT

Supporting Information. Experimental details. This material is available free of charge via the Internet at http://pubs.acs.org.

■ AUTHOR INFORMATION

Corresponding Author
strano@mit.edu

■ ACKNOWLEDGMENT

This work was supported by awards from the Beckmann Foundation and NSF to M.S.S. and from the NSF to L.K.M. (CAREER, CHE- 0644530). N.F.R. was supported by the NSF Graduate Fellowship. Glycan reagents were donated by the Consortium of Functional Glycomics and Lectin plasmids from the L. Mahal group. We would also like to acknowledge R. Raman and D. Wittrup for fruitful discussions of glycan and lectins as well as D. Heller and P. Barone for discussions of SWNT measurements.

■ REFERENCES

(1) Ohtsubo, K.; Marth, J. D. *Cell* **2006**, *126*, 855.
(2) Gamblin, D. P.; Scanlan, E. M.; Davis, B. G. *Chem. Rev.* **2009**, *109*, 131.
(3) Li, H. J.; d'Anjou, M. *Curr. Opin. Biotechnol.* **2009**, *20*, 678.
(4) Elola, M. T.; Wolfenstein-Todel, C.; Troncoso, M. F.; Vasta, G. R.; Rabinovich, G. A. *Cell. Mol. Life Sci.* **2007**, *64*, 1679.
(5) Hirabayashi, J. *J. Biochem.* **2008**, *144*, 139.
(6) Hirabayashi, J.; Kuno, A.; Tateno, H. *Electrophoresis* **2011**, *32*, 1118.
(7) Harvey, D. J. *Proteomics* **2001**, *1*, 311.
(8) Cortes, D. F.; Kabulski, J. L.; Lazar, A. C.; Lazar, I. M. *Electrophoresis* **2011**, *32*, 14.

(9) Lazar, I. M.; Lazar, A. C.; Cortes, D. F.; Kabulski, J. L. *Electrophoresis* **2011**, *32*, 3.
(10) Pilobello, K. T.; Krishnamoorthy, L.; Slawek, D.; Mahal, L. K. *ChemBioChem* **2005**, *6*, 985.
(11) Zheng, T.; Peelen, D.; Smith, L. M. *J. Am. Chem. Soc.* **2005**, *127*, 9982.
(12) Rosenfeld, R.; Bangio, H.; Gerwig, G. J.; Rosenberg, R.; Aloni, R.; Cohen, Y.; Amor, Y.; Plaschkes, I.; Kamerling, J. P.; Maya, R. B. Y. *J. Biochem. Biophys. Methods* **2007**, *70*, 415.
(13) Tao, S. C.; Li, Y.; Zhou, J. B.; Qian, J.; Schnaar, R. L.; Zhang, Y.; Goldstein, I. J.; Zhu, H.; Schneck, J. P. *Glycobiology* **2008**, *18*, 761.
(14) Liang, P. H.; Wang, S. K.; Wong, C. H. *J. Am. Chem. Soc.* **2007**, *129*, 11177.
(15) Ahn, J. H.; Kim, J. H.; Reuel, N. F.; Barone, P. W.; Boghossian, A. A.; Zhang, J.; Yoon, H.; Chang, A. C.; Hilmer, A. J.; Strano, M. S. *Nano Lett* **2011**, *11*, 2743.
(16) Weis, W. I.; Drickamer, K. *Annu. Rev. Biochem.* **1996**, *65*, 441.
(17) Wijagkanalan, W.; Kawakami, S.; Hashida, M. *Front. Biosci.* **2011**, *17*, 2970.
(18) Hong, S. Y.; Tobias, G.; Al-Jamal, K. T.; Ballesteros, B.; Ali-Boucetta, H.; Lozano-Perez, S.; Nellist, P. D.; Sim, R. B.; Finucane, C.; Mather, S. J.; Green, M. L. H.; Kostarelos, K.; Davis, B. G. *Nat. Mater.* **2010**, *9*, 485.
(19) Vedala, H.; Chen, Y. A.; Cecioni, S.; Imberty, A.; Vidal, S.; Star, A. *Nano Lett.* **2011**, *11*, 170.
(20) Nagaraj, V. J.; Aithal, S.; Eaton, S.; Bothara, M.; Wiktor, P.; Prasad, S. *Nanomedicine* **2010**, *5*, 369.
(21) Xue, Y.; Bao, L.; Xiao, X.; Ding, L.; Lei, J.; Ju, H. *Anal. Biochem.* **2011**, *410*, 92.
(22) Varki, A. *Essentials of glycobiology*, 2nd ed.; Cold Spring Harbor Laboratory Press: Cold Spring Harbor, NY, 2009.
(23) Larsen, K.; Thygesen, M. B.; Guillaumie, F.; Willats, W. G. T.; Jensen, K. J. *Carbohydr. Res.* **2006**, *341*, 1209.
(24) Stevens, J.; Blixt, O.; Paulson, J. C.; Wilson, I. A. *Nat. Rev. Microbiol.* **2006**, *4*, 857.
(25) Hagiwara, K.; Colletcassart, D.; Kobayashi, K.; Vaerman, J. P. *Mol. Immunol.* **1988**, *25*, 69.
(26) Bao, Y.; Newburg, D. S. *Electrophoresis* **2008**, *29*, 2508.
(27) Gupta, G.; Gemma, E.; Oscarson, S.; Surolia, A. *Glycoconjugate J.* **2008**, *25*, 797.
(28) Tomme, P.; Creagh, A. L.; Kilburn, D. G.; Haynes, C. A. *Biochemistry* **1996**, *35*, 13885.
(29) Tateno, H.; Nakamura-Tsuruta, S.; Hirabayashi, J. *Nat. Protoc.* **2007**, *2*, 2529.
(30) Zhang, Y. L.; Li, Q. A.; Rodriguez, L. G.; Gildersleeve, J. C. *J. Am. Chem. Soc.* **2010**, *132*, 9653.
(31) Oyelaran, O.; Li, Q.; Farnsworth, D.; Gildersleeve, J. C. *J. Proteome Res.* **2009**, *8*, 3529.
(32) Karamanska, R.; Clarke, J.; Blixt, O.; MacRae, J. I.; Zhang, J. Q.; Crocker, P. R.; Laurent, N.; Wright, A.; Flitsch, S. L.; Russell, D. A.; Field, R. A. *Glycoconjugate J.* **2008**, *25*, 69.
(33) Hsu, K. L.; Gildersleeve, J. C.; Mahal, L. K. *Mol. BioSyst.* **2008**, *4*, 654.
(34) Wittig, I.; Schagger, H. *Proteomics* **2005**, *5*, 4338.
(35) Zhang, J. Q.; Boghossian, A. A.; Barone, P. W.; Rwei, A.; Kim, J. H.; Lin, D. H.; Heller, D. A.; Hilmer, A. J.; Nair, N.; Reuel, N. F.; Strano, M. S. *J. Am. Chem. Soc.* **2011**, *133*, 567.
(36) Boghossian, A. A.; Zhang, J.; Floch, F. T. L.; Ulissi, Z. W.; Bojo, P.; Han, J.-H.; Kim, J.-H.; Arkalgud, J. R.; Reuel, N. F.; Braatz, R.; Strano, M. S. *J. Chem. Phys.* **2011**, 135.
(37) Ahmed, H. *Principles and reactions of protein extraction, purification, and characterization*; CRC Press: Boca Raton, FL, 2005.
(38) Brege, J. J.; Gallaway, C.; Barron, A. R. *J. Phys. Chem. C* **2009**, *113*, 4270.
(39) Jin, H.; Jeng, E. S.; Heller, D. A.; Jena, P. V.; Kirmse, R.; Langowski, J.; Strano, M. S. *Macromolecules* **2007**, *40*, 6731.
(40) Oshannessy, D. J.; Brighamburke, M.; Soneson, K. K.; Hensley, P.; Brooks, I. *Anal. Biochem.* **1993**, *212*, 457.
(41) Nieba, L.; NiebaAxmann, S. E.; Persson, A.; Hamalainen, M.; Edebratt, F.; Hansson, A.; Lidholm, J.; Magnusson, K.; Karlsson, A. F.; Pluckthun, A. *Anal. Biochem.* **1997**, *252*, 217.
(42) Perret, S.; Sabin, C.; Dumon, C.; Pokorna, M.; Gautier, C.; Galanina, O.; Ilia, S.; Bovin, N.; Nicaise, M.; Desmadril, M.; Gilboa-Garber, N.; Wimmerova, M.; Mitchell, E. P.; Imberty, A. *Biochem. J.* **2005**, *389*, 325.
(43) Yoon, H.; Ahn, J. H.; Barone, P. W.; Yum, K.; Sharma, R.; Boghossian, A. A.; Han, J. H.; Strano, M. S. *Angew. Chem., Int. Ed.* **2011**, *50*, 1828.
(44) Saarela, S.; WesterlundWikstrom, B.; Rhen, M.; Korhonen, T. K. *Infect. Immun.* **1996**, *64*, 2857.
(45) Tanskanen, J.; Saarela, S.; Tankka, S.; Kalkkinen, N.; Rhen, M.; Korhonen, T. K.; Westerlund-Wikstrom, B. *J. Bacteriol.* **2001**, *183*, 512.
(46) Merckel, M. C.; Tanskanen, J.; Edelman, S.; Westerlund-Wikstrom, B.; Korhonen, T. K.; Goldman, A. *J. Mol. Biol.* **2003**, *331*, 897.
(47) Carrillo, L. D.; Krishnamoorthy, L.; Mahal, L. K. *J. Am. Chem. Soc.* **2006**, *128*, 14768.
(48) Jin, H.; Heller, D. A.; Kim, J. H.; Strano, M. S. *Nano Lett.* **2008**, *8*, 4299.
(49) Jin, H.; Heller, D. A.; Kalbacova, M.; Kim, J. H.; Zhang, J. Q.; Boghossian, A. A.; Maheshri, N.; Strano, M. S. *Nat. Nanotechnol.* **2010**, *5*, 302.
(50) Kim, J. H.; Heller, D. A.; Jin, H.; Barone, P. W.; Song, C.; Zhang, J.; Trudel, L. J.; Wogan, G. N.; Tannenbaum, S. R.; Strano, M. S. *Nat. Chem.* **2009**, *1*, 473.
(51) Heller, D. A.; Pratt, G. W.; Zhang, J. Q.; Nair, N.; Hansborough, A. J.; Boghossian, A. A.; Reuel, N. F.; Barone, P. W.; Strano, M. S. *Proc. Natl. Acad. Sci. U.S.A.* **2011**, *108*, 8544.
(52) Reuel, N. F.; Bojo, P.; Zhang, J.; Boghossian, A. A.; Ahn, J.-H.; Kim, J.-H.; Strano, M. S. *Bioinformatics* (submitted).
(53) Chung, S. H.; Kennedy, R. A. *J. Neurosci. Methods* **1991**, *40*, 71.